Tanzania Journal of Engineering and Technology 2025, **44**(3):49-68
OPEN ACCESS articles distributed under Creative Commons Attribution Licence [CC BY-ND]
Websites: https://commons.udsm.ac.tz/tjet/; https://ajol.org/tjet

ISSN 1821-536X (**print**); ISSN 2619-8789 (**electronic**)
https://doi.org/10.52339/tjet.v44i3.1241

Regular Research Manuscript

Techno-Economic Analysis of Hybrid PV-Wind-Diesel Generator Swarm Grid for Rural Electrification in Tanzania

Ibrahim A. Mwammenywa[1†], Joseph S. Mwakijale[1,2], and Monish Krishna[2]

[1]Department of Electrical Engineering, University of Dar es Salaam, Dar es Salaam, Tanzania
[2] Sensor Technology Department, Paderborn University, Paderborn, Germany
[†]Corresponding Author: ibrahim.mwammenywa@udsm.ac.tz; ORCID: 0000-0003-2735-643X

ABSTRACT

Remote, rural, and off-grid communities, particularly in Sub-Saharan Africa (SSA), face significant challenges in securing reliable and affordable electricity. While solutions such as solar home systems (SHSs) and diesel generators (DGs) have been adopted by some individuals, their deployment is often not optimized to meet the full load demand. This study addresses this challenge by proposing a hybrid swarm grid (HSG) design that integrates photovoltaic (PV), wind energy, and diesel generators (DGs). Utilizing MATLAB/Simulink and HOMER, the HSG is modeled and optimized for a typical SSA village, incorporating real-world variables such as load demand profiles, solar irradiance, and wind patterns. A comprehensive techno-economic analysis is conducted to evaluate the feasibility and effectiveness of the proposed system, taking into account equipment, fuel, and maintenance costs. The HSG configuration yields a Levelized Cost of Energy (LCoE) of €0.123 /kWh (TZS 344.4 /kWh), which is significantly lower than the average LCoE of €0.375 /kWh (TZS 1,050 /kWh) for individual systems. This highlights the potential of hybrid-based swarm grids to deliver cost-effective energy solutions, even in applications with high demand from multiple consumers. Furthermore, this research provides strong evidence for prosumers to invest in renewable-based swarm grids over conventional diesel generators, which exhibit higher Net Present Costs (NPC), LCoE, and environmental impact.

ARTICLE INFO
Submitted: **May 20, 2025**
Revised: **Aug. 30, 2025**
Accepted: **Sep. 9, 2025**
Published: **Oct. 2025**

Keywords: *Swarm Grid, Hybrid Energy System, Renewable Energy Sources (RESs), MATLAB/Simulink, HOMER energy*.

INTRODUCTION

Most of the population in the Global South lacks access to clean, reliable, and affordable energy, particularly electricity. In Sub-Saharan Africa (SSA), this challenge is acute, with approximately 600 million people (about 53% of the population) lacking electricity access (Amui & Commodities Branch, 2023). In response, SSA governments are actively pursuing the United Nations Sustainable Development Goal 7 (UNSDG7), which aims to *ensure universal access to affordable, sustainable, and clean energy* by 2030 (United Nations, 2015). To achieve this goal, various strategies have been considered, including the deployment of microgrids, individual energy solutions, and the extension of national grids into rural areas (Bowes et al., 2017). However, extending national grids faces significant challenges, such as the high cost of

constructing long transmission lines and substantial power losses. These issues are exacerbated by the dispersed nature of rural communities, which are often located far from urban centers (Peters et al., 2019). While microgrids offer a promising alternative, their widespread adoption has been limited by high upfront investment costs, which often lead to unaffordable electricity for impoverished rural communities. Furthermore, many existing microgrids are failing due to a number of factors, including customer dropouts, political interference, and a lack of technical and project management skills within these communities (Namujju et al., 2024; Bogere & Temmen, 2024).

Conversely, some individuals in rural communities have increasingly adopted solar home systems (SHSs) and small diesel generators (DGs) to secure electricity access (Clancy, 2025). The growing uptake of SHSs can be attributed to the global decline in solar photovoltaic (PV) module prices, making these systems a more financially accessible solution. Nevertheless, these individual systems, particularly SHSs, are often not optimized for the local load demand. Specifically, the self-consumption of PV-generated energy is low due to the inherent volatility and intermittency of solar resources. As a result, SHSs may produce a surplus of energy during the day that goes unutilized, while failing to satisfy the community's energy demand during evening and nighttime hours (Groh et al., 2014). This disparity highlights a significant opportunity: surplus energy could be either traded among community members or stored in a centralized, community-based energy storage system for later use.

Nevertheless, individual SHSs and their associated storage systems can be interconnected to form a small, decentralized mini-grid known as a swarm grid (Soltowski et al., 2019). This configuration allows for the sharing and optimal utilization of individual resources within a community. By leveraging the complementary load demand profiles and diverse generation and storage capacities of prosumers and consumers, a swarm grid enhances electricity access and availability without the need for significant new generation or storage infrastructure (Hoffmann & Ansari, 2019).

Swarm grids are emerging as a promising and viable approach for rural electrification, particularly in Sub-Saharan Africa. Their ad-hoc nature allows them to grow organically from existing individual resources, expanding as more become available. This makes them highly suitable for rural communities with limited capital, offering a more flexible alternative to extending national grids or developing a full-scale microgrid (Sheridan et al., 2023). A swarm grid can grow incrementally and eventually be integrated into a larger microgrid or the national grid without requiring a substantial upfront investment (Hoffmann & Ansari, 2019).

This paper assesses the potential of hybrid swarm grids (HSGs), focusing on the effective utilization of generated electricity and the Levelized Cost of Energy (LCoE). A hybrid model, which integrates diverse prosumers with solar PVs, wind turbines, DGs, and energy storage, has been developed. The primary aim of this model is to provide a reliable and environmentally sustainable power supply, mitigating the impact of weather variability and reducing reliance on fossil fuels. The model is implemented in MATLAB/Simulink R2023b (MATLAB, 2021) using 24-hour real-world data with a one-hour time resolution to examine the energy sharing possibilities among prosumers and consumers. HOMER software is then employed to optimize the designed models and analyze their cost-effectiveness across various scenarios.

The rest of this paper is organized as follows: Section 2 provides a literature review of related works. Section 3 describes the proposed system architecture and modelling. Section 4 presents the simulation results and discussion of

different SG configurations. A financial analysis is presented in Section 5. Finally, Section 6 summarizes the key findings of this research.

RELATED WORKS

Various studies have explored the implementation of swarm grids. Much of this research has focused on utilizing renewable sources within mini- or microgrid configurations, with some investigations addressing technological advancements in the development of swarm grids.

The study by Hoffmann & Ansari (2019) investigated the potential of establishing swarm grids in communities that are already connected to a national grid. Their work demonstrated the potential for reducing energy costs by optimally balancing energy drawn from the national grid with electricity supplied by individual prosumers. However, a significant limitation of their analysis is that it does not extend to unelectrified rural communities located far from the national grid, where grid extension is not a viable option. Furthermore, the study's scope is restricted to the integration of only SHSs and DGs, neglecting to explore the potential of integrating hybrid renewable energy sources, such as PV-wind systems.

Giraneza et al. (2021) proposed a centralized energy storage system, referred to as an "energy bank" for use within a swarm grid. In their model, the centralized energy bank connects both prosumers and consumers, storing surplus energy and responding to energy demand requests. In cases of energy request contention, priority is given to prosumers. While the study provides a robust formulation of the centralized storage system, it fails to address critical issues such as billing, security, and privacy. Furthermore, the concept of a centralized storage bank lacks practical feasibility in sparsely populated villages due to the high cost of connecting each stakeholder and the significant transmission losses experienced by distant participants. The operational and management costs of the centralized storage have also not been discussed.

In addressing the technical challenges of forming swarm grids (SGs), Mwakijale et al. (2024, 2023) proposed the use of smart transceivers for energy management, billing, and dispatch control. A key limitation of this work, however, is that the transceiver's operation is restricted to solar-only swarm grids. The study also does not address how multiple simultaneous requests are handled to prevent imbalances within the SG. In related work, Mwakijale & Hilleringmann (2024) discussed the impact of various threshold parameters on the choice between AC and DC distribution lines. The authors used factors such as conductor size, household separation distance, conductor characteristics, shared power, and converter losses (including power factor losses for AC) to determine power loss for each distribution type. A threshold was subsequently derived to guide the selection of either an AC or DC distribution line. Despite this, the study did not consider the implementation costs of each distribution line or the market availability of AC and DC appliances, which are critical factors for a comprehensive conclusion.

The EU project technology (Swarm-E, 2025) provides a comprehensive real-world evaluation of swarm grid systems. The project showcases scalable deployments in countries such as Tanzania and Bangladesh, emphasizing modularity, peer-to-peer electricity trading, affordability, and integration with productive-use technologies like e-mobility charging and cold storage. Economically, the system is designed to be accessible, with users paying a one-time fee for a controller and then participating in energy trading via digital platforms-demonstrating a practical balance between technical innovation and financial inclusivity.

Therefore, this work addresses the techno-economic viability of implementing SGs in SSA. It seeks to answer the primary

research question: How economically feasible is it for rural communities to share electrical energy through SGs.

SYSTEM ARCHITECTURE AND MODELLING

Figure 1 illustrates the proposed swarm grid architecture developed for this study. The model represents a hypothetical community of four prosumers: a commercial entity with a DG, a residential household with a small wind turbine, and two households with solar home systems (SHSs) coupled with battery storage. In this architecture, solar PVs and wind generators serve as the primary energy sources, with the DG optimized for backup. To maximize the benefits of the swarm grid, all generated energy is shared among prosumers with battery storage, irrespective of its origin.

Weather Data

For this study, average weather data for Tanzania, spanning from 2018 to 2023, were obtained from NASA (NASA - Langley Research Center, 2024) and SOLCAST (Solcast, 2025). The dataset, which includes solar irradiance, temperature, and wind speed, was thoroughly analyzed and applied as input for the simulations in this study. Solar irradiance and temperature are critical factors influencing the electricity generated by solar PVs, whereas wind speed is directly proportional to the power output of the wind turbine. The seasonal variation of these weather parameters is presented in Figure 2.

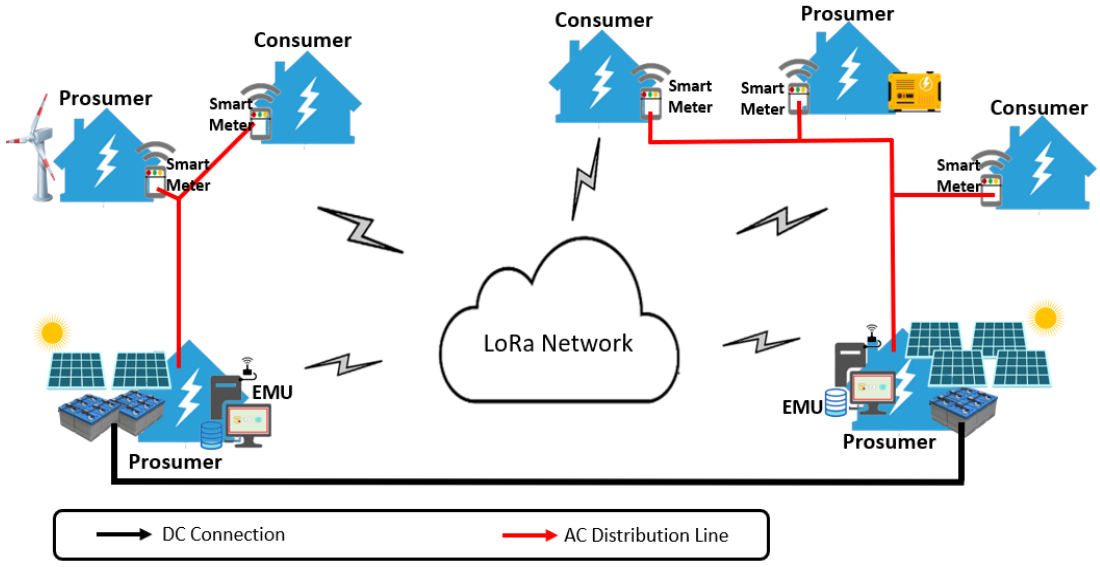

Figure 1: Swarm grid system architecture (Mwakijale et al., 2023).

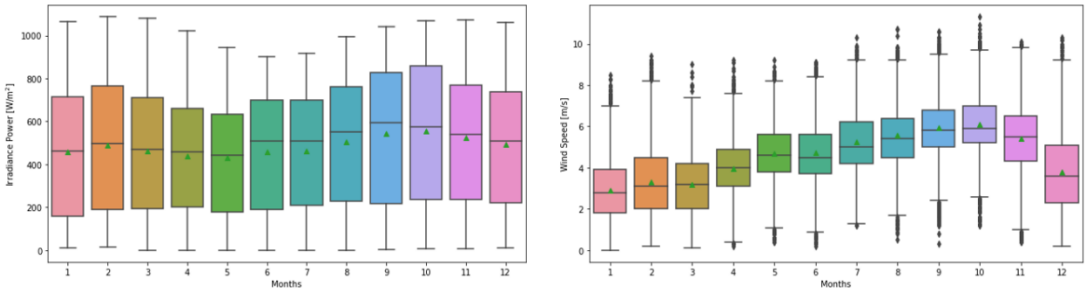

Figure 2: The monthly data of global irradiance and wind speed in Tanzania.

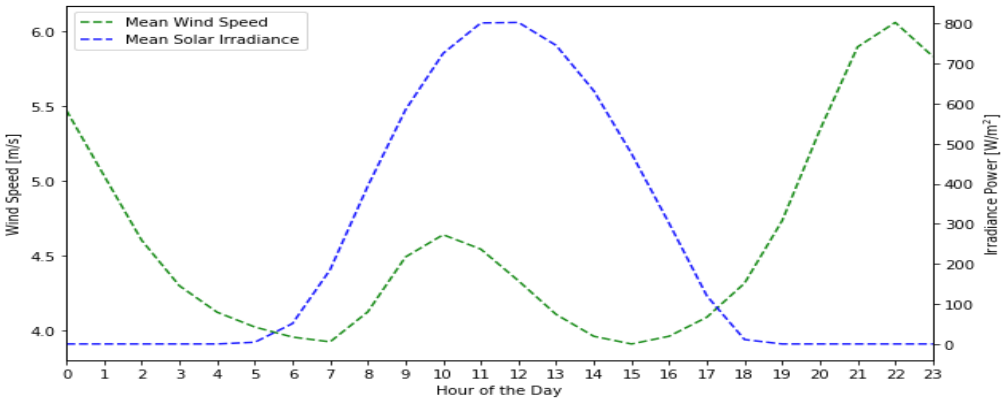

Figure 3: Mean hourly solar irradiation and wind speed.

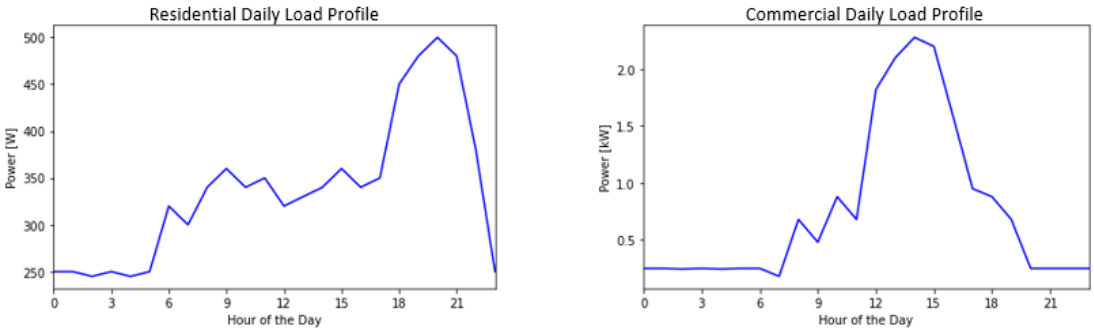

Figure 4: Mean daily load profiles in a proposed swarm grid.

According to Figure 2, there is a consistent potential for electricity generation from both solar and wind sources throughout the year. The mean monthly global solar irradiance ranges from 500 – 600 W/m², while the mean monthly wind speed is between 3 – 5 m/s. The consistent high solar irradiance indicates its viability as a primary source of electricity in rural villages. Figure 3 shows the mean daily distribution of solar irradiance and wind energy potential. Peak solar irradiance approximately reaches 800 W/m², while the average wind speed is 4 m/s. Notably, wind and solar resources offer complementary patterns for electricity generation.

Load Profiles

Load profile data, sourced from Mwammenywa & Hilleringmann (2023), Philipo et al. (2020), and Williams et al. (2018), were used to model the residential and commercial loads in this study.The mean daily load profiles for residential and commercial prosumers are shown in Figure 4. Consistent with an equitable energy access approach, as described by Hoffmann & Ansari (2019), residential prosumers and consumers are assumed to share a similar load profile.

Description of Partial Models

Solar PV System Model

The solar cell illustrated in Figure 5, utilizes the Bellini model (Bellini et al., 2009). The actual PV current I_P depends on the actual PV voltage output V_P and other parameters K_1 and K_2, according to the following mathematical equations:

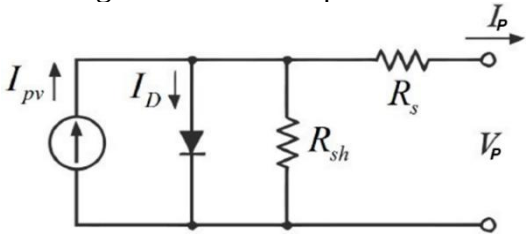

Figure 5: Equivalent circuit of the PV cell (Source: Bellini et al., 2009).

$$I_P = I_{SC} \cdot \left[1 - K_1 . \left(e^{\left(\frac{V_P}{K_2 \cdot V_{OC}}\right)} - 1\right)\right] \quad (1)$$

$$K_1 = \left(1 - \frac{I_{MPP}}{I_{SC}}\right) \cdot e^{\left(\frac{-V_{MPP}}{K_2 \cdot V_{OC}}\right)} \quad (2)$$

$$K_2 = \frac{\left(\frac{V_{MPP}}{V_{OC}} - 1\right)}{ln\left(1 - \frac{I_{MPP}}{I_{SC}}\right)} \quad (3)$$

Parameters K_1 and K_2 depend on irradiance G and temperature T at a given time. Variations in irradiance and temperature affect the short circuit current I_{SC}, open circuit voltage V_{OC}, maximum power point voltage V_{MPP} and maximum power point current I_{MPP}; as described in the following equations:

$$I_{SC}(G,T) = I_{SCS}\frac{G}{G_S}[1 + \alpha(T - T_S)] \quad (4)$$

$$V_{OC}(T) = V_{OCS} + \beta(T - T_S) \quad (5)$$

$$I_{MPP}(G,T) = I_{MPPS}\frac{G}{G_S}[1 + \alpha(T - T_S)] \quad (6)$$

$$V_{MPP}(T) = V_{MPPS} + \beta(T - T_S) \quad (7)$$

Current parameters are influenced by solar irradiance and temperature, whereas voltage parameters are temperature-depend only. I_{SCS}, I_{MPPS}, V_{OCS} and V_{MPPS} are short circuit and maximum power point currents, and open circuit and maximum power point voltages of a solar PV, respectively, at standard test conditions (STC: G_S =1000 W/m^2 and T_S =25 ˚C = 298.15 K). α and β are current and voltage temperature coefficients, respectively, as per the manufacturers' module datasheet, provided in Table 1.

In this study, maximum power point voltage V_{MPP} and current I_{MPP} are taken as the output voltage and current of the single PV module. The PV system's power output is calculated by multiplying the output current by the number of parallel strings and the output voltage by the number of modules in series within each string. The incremental conductance (INC) maximum power point tracking (MPPT) technique is implemented for PV system simulation. The INC MPPT algorithm, utilizing a boost converter, offers flexibility, real-time response, and simplicity compared to other MPPT algorithms (Mohamed & Abd El Sattar, 2019). Figure 6 illustrates the INC MPPT algorithm, which dynamically adjusts the PV's operating point to maintain operation at the maximum power point (MPP).

Table 1: PV system characteristics

PV Characteristics	Values
Maximum Power Point at STC [P_{MPP}]	250 W_p
Voltage at Maximum Power Point [V_{MPP}]	30.7 V
Current at Maximum Power Point [I_{MPP}]	8.15 A
Short Circuit Current [I_{SC}]	8.66 A
Open Circuit Voltage [V_{OC}]	37.3 V
Temperature coefficient of I_{SC}	0.086998% /K
Temperature coefficient of V_{OC}	-0.36901% /K
No of Cells	60

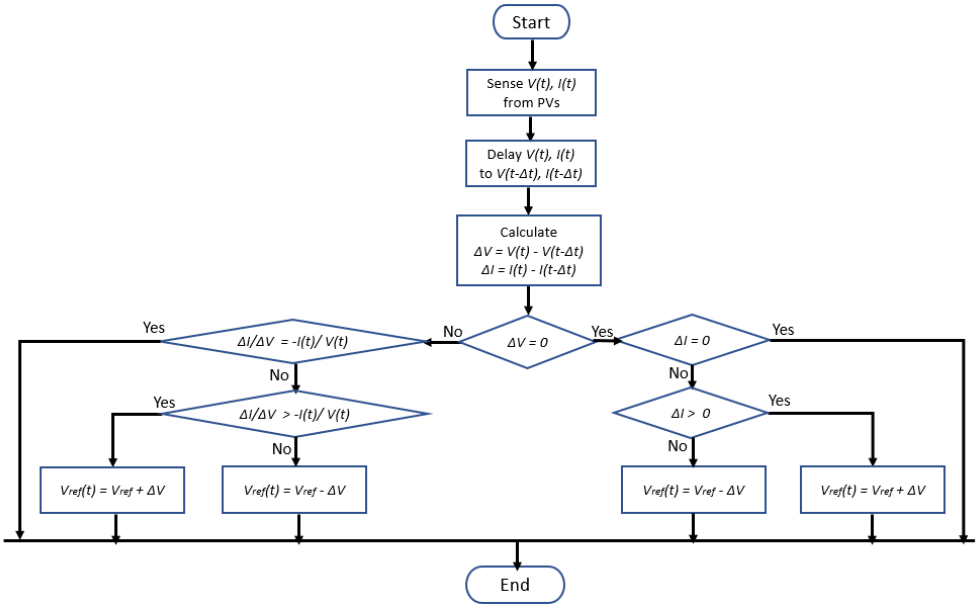

Figure 6: Incremental conductance algorithm (Mohamed & Abd El Sattar, 2019).

This study models two SHS prosumers with DC loads, as shown in Figure 1. The total PV power generation in the model, depicted in Figure 7, is derived from the combined output of these two PV systems. The output voltage from each PV system passes through a DC-DC boost converter operating at a switching frequency f, which is modeled using equations (8) - (13) with parameter values provided in Table 2.

Duty Cycle: $$D = \frac{V_{out} - V_{in}}{V_{out}} \quad (8)$$

Peak-to-peak Output Ripple Voltage: $$\Delta V_{out} = \%V_{ripple} * V_{out} \quad (9)$$

Output Current: $$I_{out} = \frac{P_{out}}{V_{out}} \quad (10)$$

Peak-to-peak Inductor Current Ripple: $$\Delta I_L = \%I_{ripple} * I_{out} \quad (11)$$

Inductor Value: $$L = V_{in} * D * (\frac{1 - D}{f * \Delta I_L}) \quad (12)$$

Capacitor Value: $$C = \frac{\Delta I_L}{f * \Delta V_{out}} \quad (13)$$

Table 2: Boost Converter with INC MPPT for PV system characteristics

Model Components	Values
Maximum Output Power [W]	500
Input Voltage [V]	30
Output Voltage [V]	48
Inductance [mH]	6.8
Capacitance [µF]	813.80
Switching Frequency [kHz]	10
Duty Cycle [D]	0.375

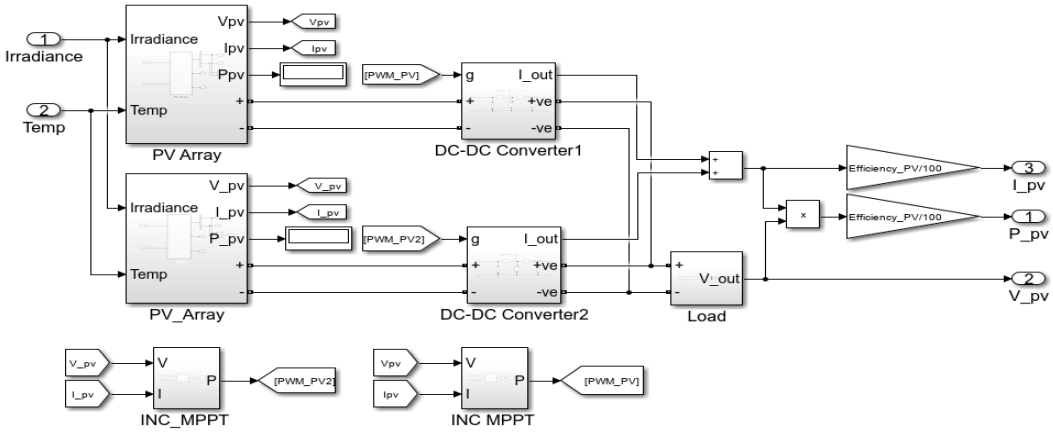

Figure 7: Layout of the PV generation in MATLAB/Simulink.

Wind Generator Model

This study integrates a Vertical Axis Wind Turbine (VAWT) power generator into the model (Justo et al., 2018). Due to their low cut-in wind speed of just 2 m/s, VAWTs are particularly well-suited for low-wind environments like Tanzania, as indicated in Figure 2 and 3. The wind system model is designed to deliver a maximum power output of 400 kW at its rated wind speed. Figure 8 illustrates the layout and model of the VAWT generator employed, and its mechanical power output, $P_{m,}$ is calculated using Equation (14).

$$P_m = C_p \rho A \, V^3 \qquad (14)$$

where C_p is the power coefficient as given the data sheet, ρ is the airflow density in Kg/m^3, A is the rotor area in m^2, and V is the air velocity in m/s.

For power conversion from mechanical P_m to electrical P_e , the turbine system is modeled with a Permanent Magnet Synchronous Generator (PMSG). This process involves the dynamics of the shaft, which converts the magnetic torque to an electrical torque. The electrical power generated is precisely defined by Equation (15). The AC output is subsequently rectified into DC using a full-wave rectifier, and a boost converter is employed to regulate the DC voltage, as depicted in

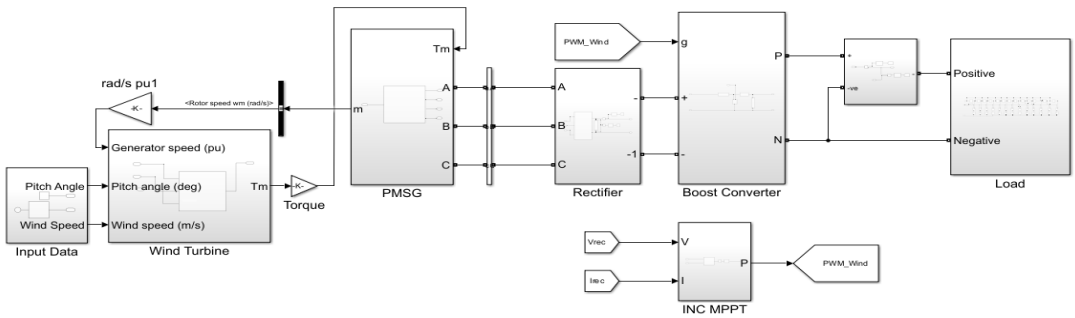

Figure 8: Layout and model of the VAWT generator in MATLAB/Simulink.

Table 3: Wind turbine system parameters

Wind Turbine Parameters	Values
Nominal Mechanical Output Power [W]	400
Base Power of Electrical Generator [VA]	400/0.9
Base Wind Speed [m/s]	3
Maximum Power at Base Windspeed (p.u)	1
Base Rotational Speed (p.u)	1.2
Pitch angle beta to display wind turbine power characteristics (*deg*)	0

Figure 8. The operational principles of the boost converter and the Incremental Conductance (INC) MPPT algorithm are further explained in Equations (8) – (13) and illustrated in Figure 6, respectively.

$$P_e = T_e.\omega_m = \frac{3}{2}p\lambda_f i_q.\omega_m \quad (15)$$

Where p is the number of poles, λ_f is the flux linkage, i_q is the q-axis stator current in Amperes, and ω_m is the mechanical angular speed in rad/s. The values of these parameters given in Table 3.

Diesel Generator Model

The DG is modeled as a diesel engine coupled to a synchronous machine as depicted in Figure 9.

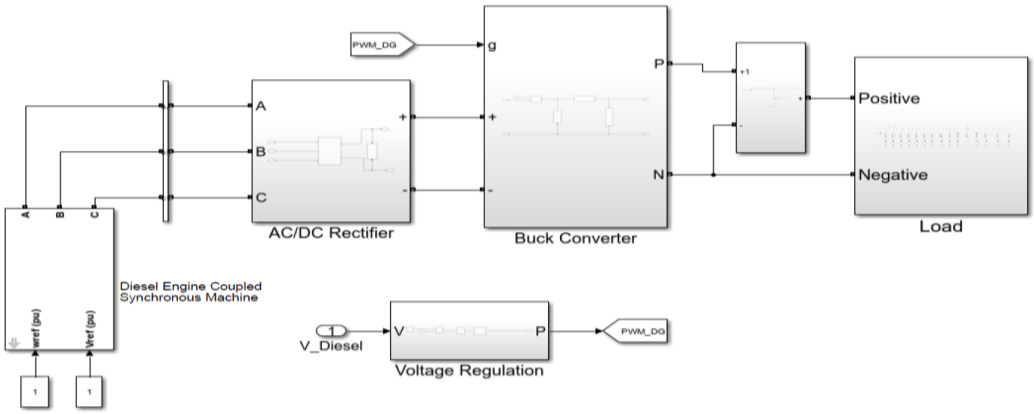

Figure 9: Diesel generator model layout in Simulink.

The synchronous generator's excitation system, a Simulink AC1A block, regulates the machine's field current using equations (16) – (18). This control mechanism manages the terminal voltage and reactive power output, which, in turn, influences voltage regulation, stability, and transient response. This system is designed to convert mechanical energy into AC power and then rectify it to DC power to power DC appliances. A DC link capacitor is used to stabilize the rectified output, minimizing voltage fluctuations. A buck converter modeled using equations (19) – (23), further adjusts the DC voltage to meet grid requirements. A proportional-integral-differential (PID) controller, governed by equations (24) – (26), regulates the voltage to a level suitable for the swarm grid by comparing the rectified output with the DC grid's standard voltage and determining the buck converter's switch duty cycle.

Mechanical Power: $$P_m = T_m.\omega \quad (16)$$

Electromagnetic Torque**:** $$T_e = \frac{3p_\tau}{2}\left(\psi_d i_q - \psi_q i_d\right) \quad (17)$$

Direct and quadrature axis Voltages: $$\begin{cases} V_d = -i_d R_d - \omega\psi_q + \dfrac{d\psi_d}{dt} \\ V_q = -i_q R_q - \omega\psi_d + \dfrac{d\psi_q}{dt} \end{cases} \quad (18)$$

Duty Cycle: $$D = \frac{V_{out}}{V_{in}} \quad (19)$$

Peak-to-peak Output Ripple Voltage**:** $$\Delta V_{out} = \%V_{ripple} * V_{out} \quad (20)$$

Peak-to-peak Inductor Current Ripple**:** $$\Delta I_L = \%I_{ripple} * I_{out} \quad (21)$$

Inductor Value**:**
$$L = (V_{in} - V_{out}) * D * (\frac{1 - D}{f * \Delta I_L}) \quad (22)$$

Capacitor Value**:**
$$C = \frac{\Delta I_L}{f * \Delta V_{out}} \quad (23)$$

Reference Voltage Comparison:
$$e(t) = v_{ref} - v_{out}(t) \quad (24)$$

PID Controller:
$$D(s) = \left(K_p + \frac{K_i}{s} + K_d s\right) E(s) \quad (25)$$

PWM Output:
$$PMW_{DG} \propto D(t) \quad (26)$$

Table 4: Synchronous Machine Parameters for Diesel Generator

Model Components	Values
Frequency	50 Hz
Rated Speed	1500 RPM
Rated Power	8.1 KVA
Rated Voltage	400 V
q-axis synchronous reactance (X_q)	0.895 pu
d-axis synchronous reactance (X_d)	1.8 pu
Stator Resistance (R_s)	0.0820 pu
Leakage Inductance (X_l)	0.072 pu
q-axis sub transient synchronous reactance (X_d'')	0.115 pu
d-axis sub transient synchronous reactance (X_q'')	0.207 pu

Table 5: Rectifier Specification for Diesel Generator

Model Parameters	Values
No. of Bridges	3
Snubber Resistance	100 Ω
Snubber Capacitance	0.1 μF
Forward Voltage (V_f)	0.8 V

Table 6: Buck Converter parameters for Diesel Generator System

Model Components	Values
Maximum Output Power [W]	3000
Input Voltage [V]	400
Output Voltage [V]	144
Inductance [mH]	16
Capacitance [μF]	926
Switching Frequency [kHz]	10
Duty Cycle [D]	0.36

where T_m is the mechanical torque, ω is the angular speed of the generator shaft, p_τ isnumber of poles, ψ_d, ψ_q are direct and quadrature axis stator flux linkage, i_q, i_d are direct and quadrature axis stator currents in Amperes, and R_d, R_q are stator resistance in d and q axes. The values of these parameters given in Tables 4 – 6.

Energy Storage Battery Model

This study models SHS prosumers that use lead-acid batteries for energy storage. The batteries store any excess energy generated by the PV system when it surpasses the current load demand. Conversely, they discharge to provide power when the load demand is higher than the generation. This storage capability is crucial for enhancing

the system's reliability and mitigating the intermittency of solar and wind energy. The battery model, shown in Figure 10, tracks the battery's state of charge (SoC), which is expressed as a percentage and is described by equations (27). The battery voltage, battery operation and charging control are modelled using equations (28) - (30) and parameter values are provided in Tables 7 and 8.

State of Charge**:**

$$SoC\ [\%] = 100\left[1 - \frac{1}{Q}\int_0^t i(t)\,dt\right] \tag{27}$$

Battery Terminal Voltage, V_{Batt} :

$$\begin{cases} E = E_0 - K\,\dfrac{Q}{Q - it} + A\,e^{-B.it} \\ V_{Batt} = E - I.R_{in} \end{cases} \tag{28}$$

Battery Operation Mode:

$$\begin{cases} Discharging\ mode:\ V_{out} = \dfrac{V_{Batt}}{1 - D} \quad D \in (0,1) \\ Charging\ mode: \qquad V_{Batt} = D.V_{in} \end{cases} \tag{29}$$

Charger Controller:

$$\begin{cases} Discharging\ mode: If\ (SoC \geq SoC_{min})\ and\ (P_{gen} < Load) \\ Charging\ mode: If\ (SoC \leq SoC_{min})\ and\ (P_{gen} > Load) \end{cases} \tag{30}$$

Table 7: Pb-Acid battery characteristics

Battery Model Parameters	Values
Rated Usable Capacity	50 Ah
Nominal terminal voltage	12 V
Maximum Charging/Discharging Current	100 A
Initial State of Charge	95 %
Maximum capacity	52 Ah
Maximum Full Charge Voltage	13.0658 V
Efficiency	95 %
Nominal discharge current	10 A
Internal Resistance	2.4 mΩ
Capacity at nominal voltage	15.5 Ah
Exponential zone	12.22 V, 0.167 Ah
Usage	On/Off-grid
Ambient Temperature	-10 °C to 50 °C

Table 8: Bidirectional Converter with INC MPPT for Battery system characteristics

Model Components	Values
Maximum Output Power [W]	500
Input Voltage [V]	12
Output Voltage [V]	48
Inductance [mH]	1.1
Boost Capacitance [µF]	813.80
Buck Capacitance [mF]	26
Switching Frequency [kHz]	10
Boost Duty Cycle [D]	0.75
Buck Duty Cycle [D]	0.25

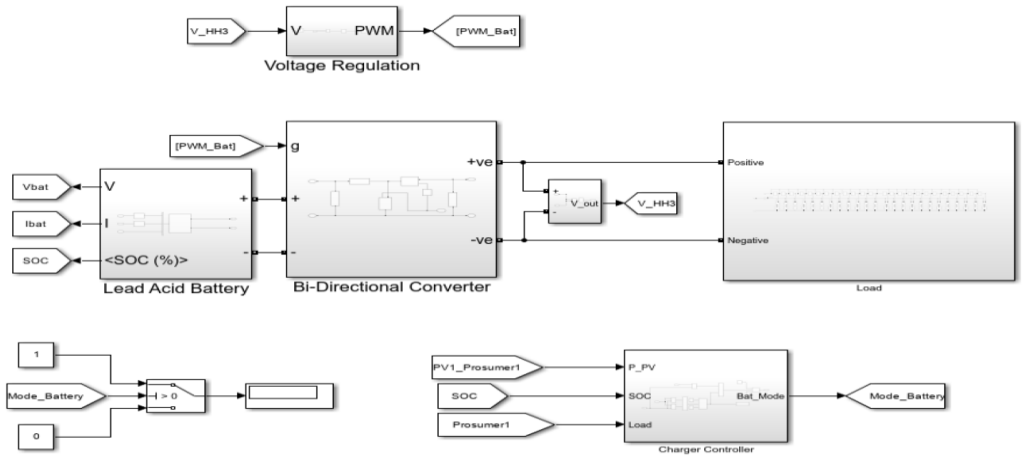

Figure 10: Pb-acid battery system model in Simulink.

The energy storage battery system in this study employs a dual-function, bidirectional DC-DC converter with a switching frequency of 20 kHz. The boost converter is governed by equations (8) – (13) and the buck converter by equations (19) – (23). A proportional-integral-differential (PID) controller modeled using equations (24) – (26), manages the converter's operation. It modulates the duty cycle of the switches by comparing the generation system's reference voltage to the battery's actual output voltage. This control strategy enables smooth transitions between voltage boost and buck modes, effectively regulating the battery's charge and discharge cycles.

Overall Swarm System Model

The swarm grid architecture depicted in Figure 1 is modeled as shown in Figure 11 and is further detailed by equations (31) – (37). Where $P_{DG,t}$ is the actual power from DG, $P_{d,i,t}$ is the power discharged from battery, $P_{c,i,t}$ is the battery charging power, D_t and C_t are battery charging and discharging states and $P_{cur,t}$ is the curtailed renewable power that cannot be stored in batteries.

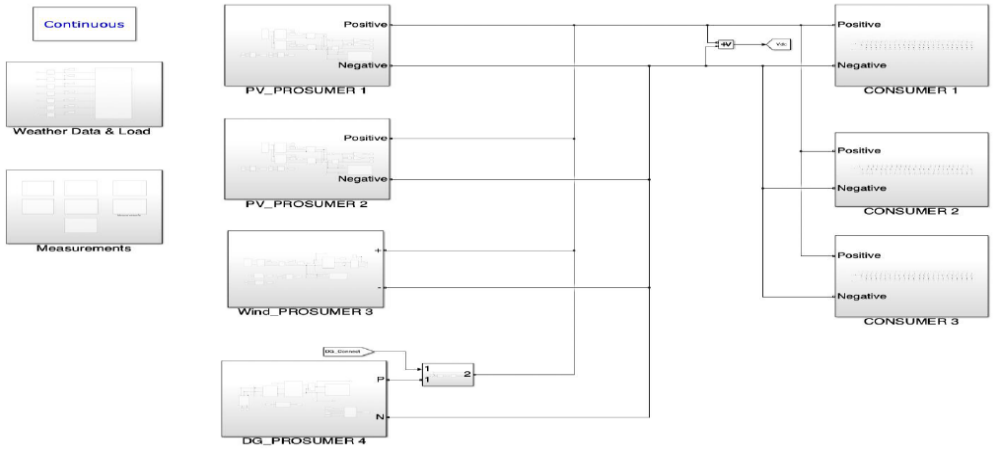

Figure 11: MATLAB/Simulink complete model for the swarm grid in this study.

Prosumers-Aggregate Power for RES:

$$P_t^{RES} = \sum_{i \in I} P_{i,t}^{RES} \tag{31}$$

Total Load (Prosumers and Consumers):

$$L_t^{tot} = \sum_{i \in I} L_{i,t} + \sum_{c \in C} L_{c,t} \tag{32}$$

$i \in I$: *Prosumers;* $c \in C$: *Consumers*

Renewable Energy Surplus:
$$\left(S_{0,t} = P_t^{RES} - L_t^{tot}\right) \geq 0 \quad (33)$$

System Power Balance:
$$P_t^{RES} + \sum_i P_{d,i,t} + P_{DG,t} = L_t^{tot} + \sum_i P_{c,i,t} + P_{cur,t} \quad (34)$$

Battery Charging Policy:
$$\sum_i P_{c,i,t} = \begin{cases} \min\left(S_{0,t},\ C_t^{max}\right), & S_{0,t} \geq 0, \\ \min\left(\max\left(0,\ P_{DG,t} - D_t\right),\ C_t^{max}\right), & S_{0,t} < 0, \end{cases} \quad (35)$$

Battery Discharging Policy:
$$\sum_i P_{d,i,t} = \min\left(-(S_{0,t}),\ D_t^{max}\right) \quad (36)$$

Curtailed Power
$$P_{cur,t} = S_{0,t} - \sum_i P_{c,i,t} \quad (37)$$

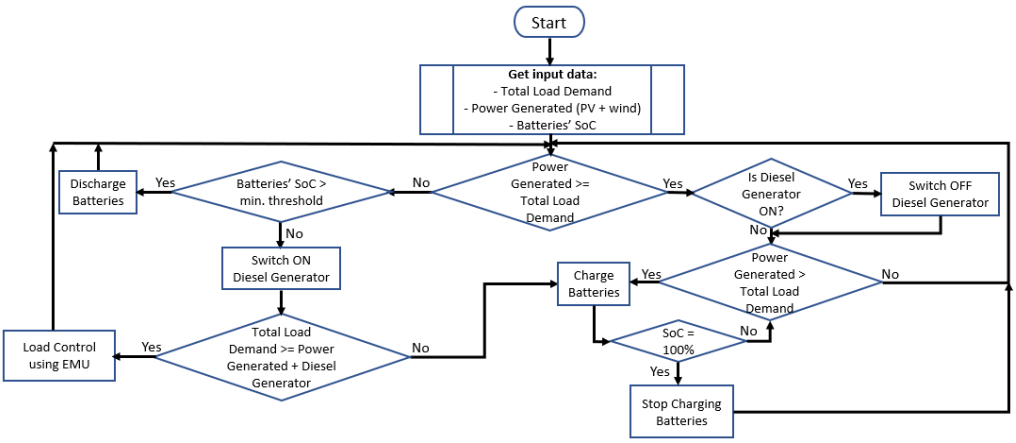

Figure 12: Flowchart of the swarm grid simulated in this study.

The model coordinates multiple prosumers-each with its own power generation and/or storage-and consumers connected via a common bus. The modeled grid has a total installed capacity of 1 kW for solar PV systems, 400 W for wind generators, and 3 kW for a diesel generator (DG). These sources are designed to collectively meet a peak load of 4.4 kW.

The system's operational strategy, illustrated in Figure 12, prioritizes the utilization of renewable energy to meet both local and shared demand. The system only draws from battery storage when renewable generation is insufficient. As a last resort, the DG is activated only when both renewable generation and battery storage are depleted.

SIMULATION RESULTS AND DISCUSSION

The proposed model was simulated using component sizing determined by HOMER to ensure optimal energy availability at the lowest system cost, based on the prosumers' load demands. Simulations were conducted over a 96-hour period, using mean daily weather data and load profiles to analyze the energy flow within the swarm grid. Four distinct cases were simulated for comparative analysis: three cases considered individual generators, while the fourth case represented the swarm grid, which utilized all three generator types.

- Individual systems, consisting of both generation and storage units (where applicable), operate independently and exclusively serve their local loads. The individual generation systems modeled in this study include:
  i. Prosumer with a SHS and energy storage system (ESS)
  ii. Prosumer with a wind system and energy storage system (ESS).
  iii. Prosumer with a DG only
- Hybrid Swarm Grid Systems: These systems consist of interconnected prosumers and consumers, facilitating

the sharing of generation and storage capacities under various control configurations.

Prosumer with a SHS and ESS

Figure 13 illustrates the performance of a prosumer with a 500 Wp solar home system (SHS) and battery storage. The system exhibits two distinct operational characteristics: a significant amount of surplus energy from 13:00 to 16:00, and an unmet energy demand during the night. The consistent operation of the SHS and the energy storage system (ESS) ensures the prosumer's daytime energy self-sufficienc

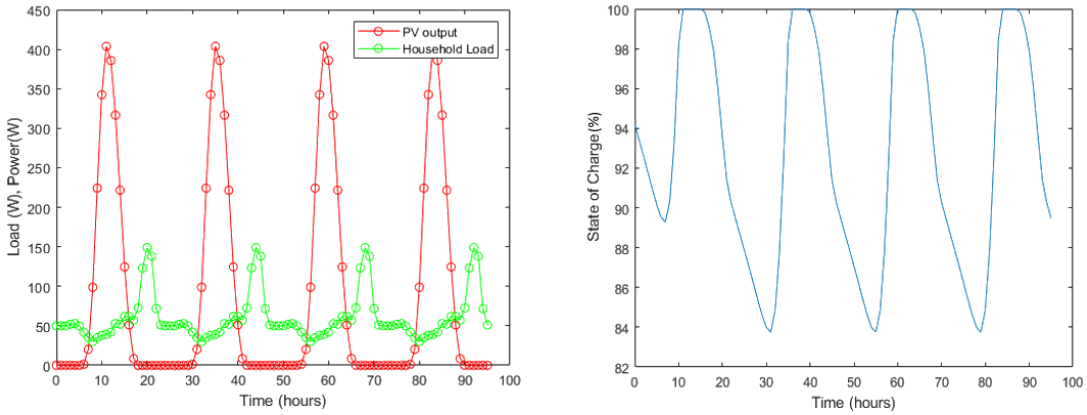

Figure 13: Generation, load and SoC profiles for a single SHS prosumer.

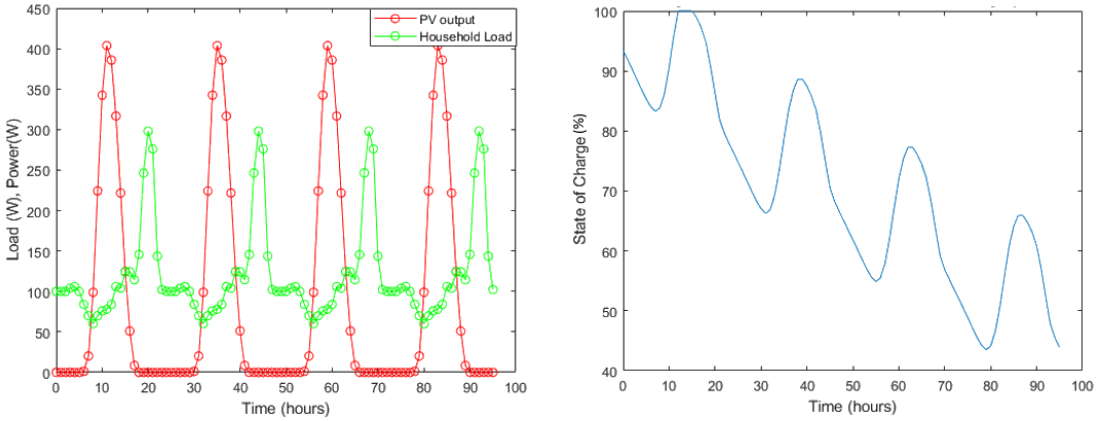

Figure 14: Generation, load and SoC profiles for a single SHS prosumer and a consumer.

by effectively meeting their local load demands. However, this configuration results in surplus energy that, if interconnected, could benefit other community members.

Figure 14 illustrates the impact of adding a consumer to the prosumer's system to utilize surplus energy. The scenario, which effectively doubles the load while maintaining the original generation and battery capacity, demonstrates that the system is unable to meet the increased demand. The additional load prevents the PV system from fully charging the battery, resulting in a continuous net discharge. This highlights the limitations of a standalone prosumer system to support additional consumers without a corresponding increase in generation or storage capacity.

Prosumer with a Wind System and ESS

Figure 15 illustrates the performance of a prosumer with a 400 Wp wind system and battery storage. In this case, the wind system consistently meets the local load demand, making the battery storage largely redundant. This outcome, however, demonstrates the potential of this system to support additional interconnected consumers, particularly during periods of off-peak generation. This highlights the

value of wind-based prosumers as a stable source of energy for a wider community.

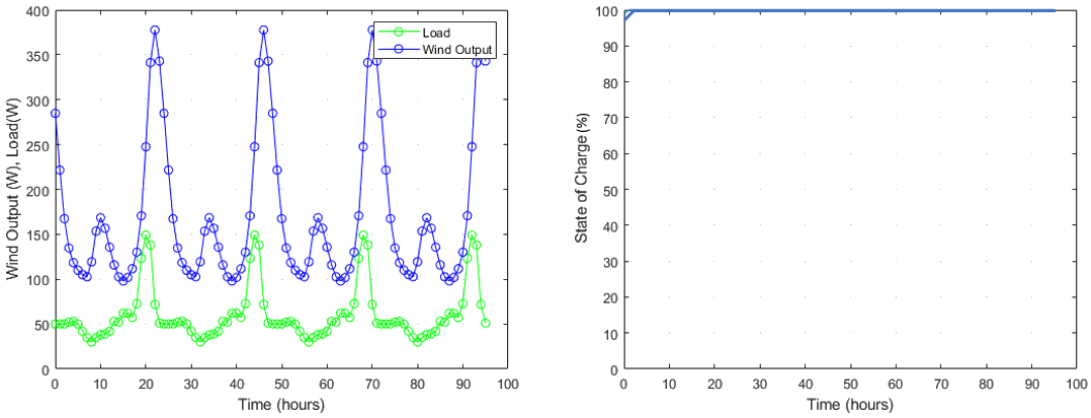

Figure 15: Generation, load and SoC profiles for a wind system prosumer.

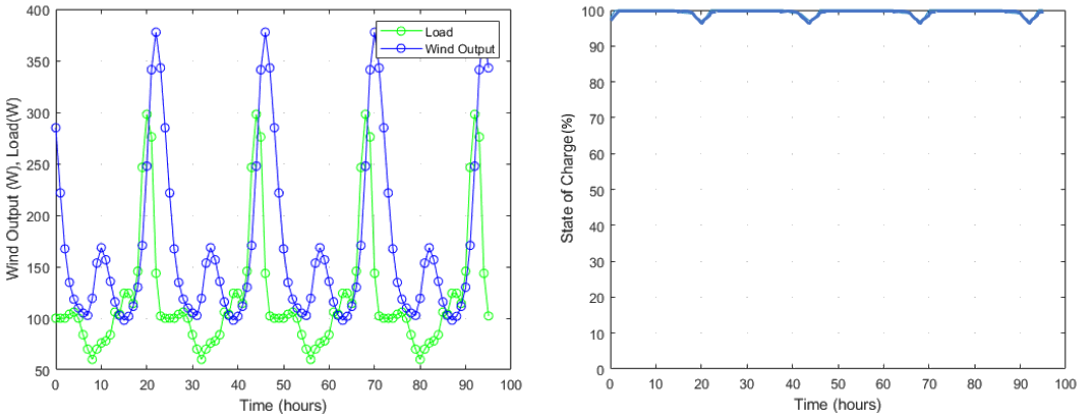

Figure 16: Generation, load and SoC profiles for a wind system prosumer with a consumer.

The wind system exhibits remarkable consistency, ensuring the prosumer's energy self-sufficiency without deficits, even without relying on a battery. This is because generation consistently surpasses load demand throughout both the day and night. However, a substantial amount of unutilized energy could be shared to benefit other interconnected community members. Figure 16 presents a simulation of the wind system with an additional consumer. The results demonstrate the system's capacity to support multiple consumers; however, with the increased load, battery storage becomes necessary to supplement energy during periods when wind generation falls below the total load demand.

Prosumer with a DG System

The DG used in this simulation has a maximum power output of 3 kW. By design, it supplies power commensurate with the load demand. However, during startup, the DG's rotational speed is elevated, resulting in a transiently higher power output. Fluctuations in demand throughout the day cause the DG to produce excess power at certain operational times, as depicted in Figure 17(a).

Figure 17(b) depicts a modified DG system that incorporates battery energy storage. This configuration stores excess DG output during periods of high operation and uses it to supply light loads, primarily at night, when the DG is switched off. The battery is recharged during midday when the DG is

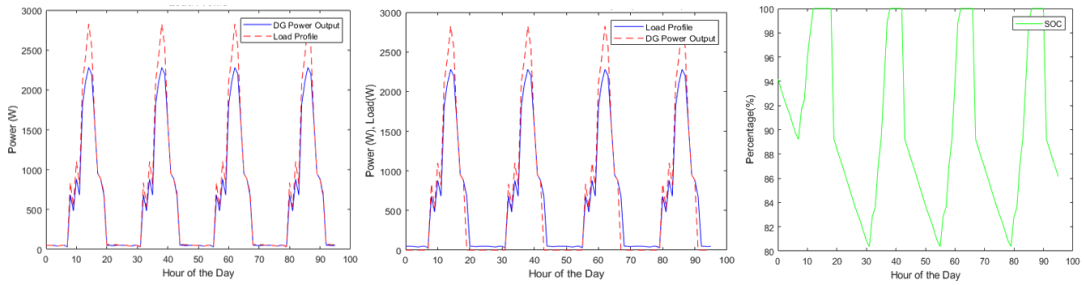

(a) (b) (c)

Figure 17: Generation, load and SoC profiles for a DG system prosumer.

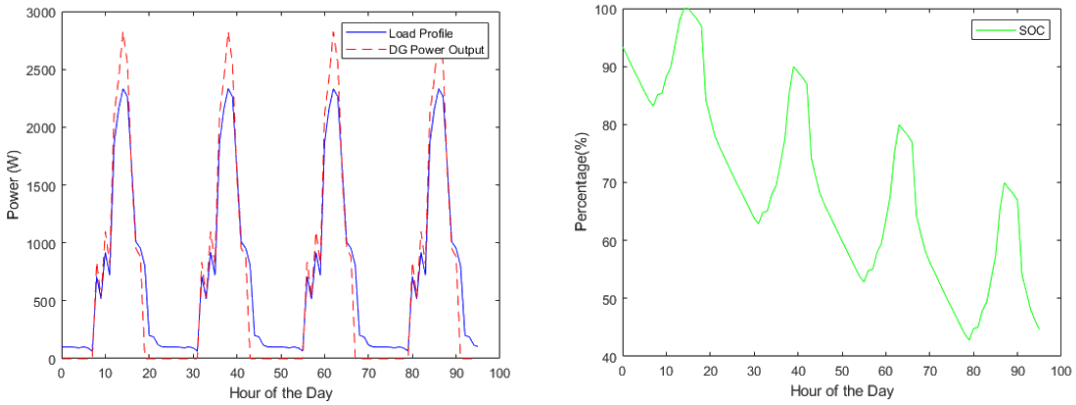

Figure 18: Supply, load and SoC profiles for a DG and battery prosumer and a consumer.

operational. This approach reduces DG runtime during periods of low demand, thereby minimizing maintenance costs. However, potential limitations include the battery's longevity under continuous cycling and the DG's inherent environmental impact from greenhouse gas emissions. While this hybrid setup partially mitigates reliance on the DG, its prolonged use still poses environmental concerns. Integrating renewable energy sources (RESs), such as solar or wind, could further reduce diesel consumption and emissions while potentially extending the battery's charging period beyond the DG's peak operational hours.

Figure 18 presents the simulation of a diesel generator (DG) and battery-equipped prosumer connected to a consumer. The DG's operational pattern remains consistent, as it is primarily used by the commercial prosumer during daytime hours. However, the battery provides energy during the evening to meet the consumer's load. The introduction of this additional load results in a continuous decline in the battery's state of charge (SoC), indicating that this configuration is unsustainable over time.

Swarm Grid Configuration

The simulated swarm grid, as depicted in Figure 11, comprised four prosumers with diverse energy sources, two solar home system (SHS) prosumers, a wind prosumer, and a diesel generator (DG) prosumer-along with three additional consumers. The results, presented in Figure 19, demonstrate that the system successfully met the local demands of the prosumers and supplied the energy needs of all three connected consumers. The integrated mix of photovoltaic (PV) and wind resources, supported by the DG, was crucial in balancing energy supply and demand. This highlights the importance of incorporating a diverse mix of renewable energy sources (RESs) and a reliable backup to accommodate fluctuating energy production and minimize the risk of energy deficits.

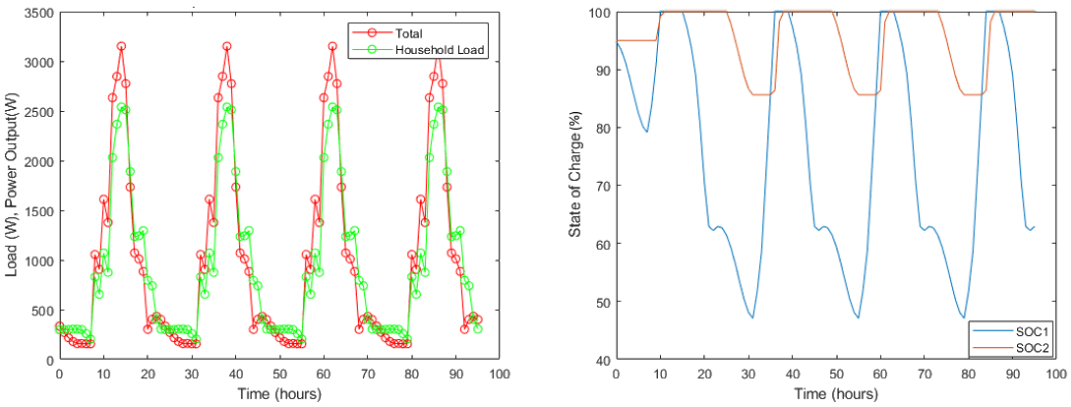

(a) (b)

Figure 19: Total power generated and load demand; and battery behaviour in a simulated swarm grid.

The results also confirm the swarm grid's efficacy in providing a reliable and continuous power supply, particularly when augmented with battery storage. Even when batteries were fully charged and the DG's operation was optimized, excess power was efficiently shared among the interconnected prosumers and consumers after local demands were met. This power-sharing mechanism minimized the waste of renewable energy generation, showcasing the system's effectiveness and economic viability.

The performance and utilization of the battery storage systems are illustrated in Figure 19(b). Battery System 1 (connected to PV Prosumer 1) was configured to discharge first, reaching a 50% depth of discharge (DoD) before Battery System 2 (connected to PV Prosumer 2) initiated discharge. This strategy, implemented on the solar prosumers (as the wind system demonstrated no need for a battery in Figure 15), was designed to minimize the charge and discharge cycles for each system. This approach also provides a crucial energy buffer for the grid during periods of low renewable energy generation. The configuration further suggests a potential to accommodate an additional consumer within the swarm grid, although this scenario was not simulated in the current study.

COST ANALYSIS

Rural electrification faces significant financial challenges, particularly with the initial investment and operational costs of renewable energy systems, which can lead to high energy prices. This study addresses this issue by analyzing two key financial indicators: Net Present Cost (NPC) and Levelized Cost of Electricity (LCOE), across four simulated cases. The NPC represents the total project cost over its lifetime, including the costs of components, transportation, installation, operation, and maintenance. LCOE, expressed as the average cost per kilowatt-hour (kWh), quantifies the affordability of electricity for each configuration.

The simulated cases from previous section were subjected to a financial analysis using equations (38) and (39), where C_0^{cap} is the initial capital expense, C_y^{cap} is the capital expense at year y, C_y^{rep}, $C_y^{O\&M}$, C_y^{fuel} are the respective replacement, operation and maintenance, and fuel costs at year y, and E_y is the total energy produced in year y. HOMER software was used to evaluate the economic viability of these configurations over a 25-year project lifespan, providing insights into their long-term cost-effectiveness, with the results summarized in Table 9.

The HSG configuration yields a LCoE of €0.123 /kWh, which is significantly lower than the average cost of €0.375 /kWh for any individual prosumer system. This is especially notable as the swarm grid serves seven users, while each individual system only serves one. This finding underscores the potential of hybrid-based swarm grids

to deliver cost-effective energy solutions for applications with high demand from multiple consumers.

The NPC of a standalone DG system is significantly high, largely due to the elevated cost of fossil fuels, frequent maintenance and repairs, and periodic replacements (Thompson Power Systems, 2024). However, when a DG is utilized as a backup or supplementary power source within the proposed swarm grid, its NPC is reduced. This reduction is a direct result of decreased fuel consumption and less frequent operation, which, in turn, lowers maintenance and repair requirements.

Net-Present Cost: $$\mathrm{NPC} = C_0^{cap} + \sum_{i \in I} \frac{C_y^{\mathrm{cap}} + C_y^{rep} + C_y^{O\&M} + C_y^{fuel}}{(1+r)^y} - S \quad (38)$$

Levelized Cost of Energy: $$\mathrm{LCoE} = \frac{NPC}{\sum_{y=1}^{N} \frac{E_y}{(1+r)^y}} \quad (39)$$

Table 9: Financial analysis and comparison

System Description	Components and Sizes	NPC (€)	Operating Cost (€/year)	LCOE (€/kWh)
Solar Home System (PV + Battery with Load)	PV – 500 W; Battery – 12 V, 50 Ah	1767	85.89	0.257
Wind System (Wind + Battery with Load)	Wind – 400 W. Battery – 12 V, 50 Ah	3057	117.34	0.445
DG Systems (DG + Battery)	DG – 3 kW Battery – 12 V, 50 Ah	43858	2809	0.54
Swarm grid system 4 Prosumers (2 SHSs + Wind + DG) and 3 extra Consumers	SHS (PV – 500 W Battery – 12 V, 50 Ah) Wind – 400 W, DG – 3 kW	6521	214.14	0.123

The analysis consistently demonstrates the economic benefits of using Renewable Energy Sources (RESs), specifically PV and wind power, which offer a lower LCoE and NPC compared to conventional DG-only systems. Furthermore, the adoption of RESs yields significant environmental advantages, including a notable reduction in carbon emissions.

CONCLUSIONS AND RECOMMENDATIONS

This study elucidates the intricate interactions among diverse energy sources, storage systems, and load profiles within a swarm grid through comprehensive simulation and analysis, providing valuable insights for practical implementation. This research contributes to the advancement of sustainable energy solutions for off-grid communities and emphasizes the transformative potential of swarm grids in shaping the future of decentralized energy systems. Swarm grids offer a promising avenue for achieving more economical, flexible, and sustainable energy solutions.

In conclusion, the simulation results underscore the viability and effectiveness of renewable energy, augmented with energy storage and strategically integrated DG backup units, in providing a reliable and sustainable energy solution for self-consumption and extended load supply. It

highlights the importance of strategic planning, energy management, and a diversified energy mix to optimize swarm grid performance, facilitating broader adoption of renewable energy systems complemented by traditional generation methods for reliable power supply in remote areas with limited access to continuous electricity (Varun, 2025).

To accommodate increased demand from additional consumers, leveraging doubled PV generation capacity and augmented storage capabilities, or incorporating additional renewable sources like wind, is essential. An intelligent management system, employing forecasting algorithms to predict demand and optimize energy distribution and storage strategies, could play a crucial role. This system would ensure optimal battery charging during peak sunlight hours and efficient energy distribution among all consumers and prosumers during high-demand periods. The simulated SoC demonstrates the system's ability to adequately supply both self-consumption and an additional consumer.

REFERENCES

Amui, R., & Commodities Branch. (2023). *Commodities at a glance: Special issue on access to energy in sub-Saharan Africa*. United Nations Conference on Trade and Development. https://shop.un.org

Anthony, M., Prasad, V., Kannadasan, R., Mekhilef, S., Alsharif, M. H., Kim, M. K., … & Aly, A. A. (2021). Autonomous fuzzy controller design for the utilization of hybrid PV-wind energy resources in demand side management environment. *Electronics*, *10*(14), 1618. doi: 10.3390/electronics10141618

Bellini, A., Bifaretti, S., Iacovone, V., & Cornaro, C. (2009). Simplified model of a photovoltaic module. In *Proceedings of the Applied Electronics* (pp. 47–51). Pilsen, Czech Republic.

Bogere, P., & Temmen, K. (2024). A Didactic Framework for Microgrids Knowledge Transfer – The Case of East Africa. In *2024 IEEE Global Engineering Education Conference (EDUCON)* (pp. 1-5). IEEE. doi:10.1109/EDUCON60312.2024.10578914

Bowes, J., Booth, C., & Strachan, S. (2017). System interconnection as a path to bottom-up electrification. *2017 52nd International Universities Power Engineering Conference, UPEC 2017, 2017-January*. doi:10.1109/UPEC.2017.8232018

Clancy, J. (2025). Energy and Low-Income Households. In *Engendering the Energy System: Looking Back to Go Forward* (pp. 75-122). Cham: Springer Nature Switzerland. doi:10.1007/978-3-031-78965-6_3

Giraneza, M., Abo-Al-Ez, K. M., & Kahn, M. T. (2021). Nanogrid Based Energy Trading System for a Rural Off-Grid Community in Africa. SSRN Electronic Journal. doi:10.2139/ssrn.3735389

Groh, S., Philipp, D., Lasch, B. E., & Kirchhoff, H. (2014, July 21). Swarm electrification-suggesting a paradigm change through building microgrids bottom-up. *Proceedings of 2014 3rd International Conference on the Developments in Renewable Energy Technology, ICDRET 2014*. doi:10.1109/icdret.2014.6861710

Hoffmann, M. M., & Ansari, D. (2019). Simulating the potential of swarm grids for pre-electrified communities–A case study from Yemen. *Renewable and Sustainable Energy Reviews*, *108*, 289-302. doi:/10.1016/j.rser.2019.03.042

Justo, J. J., Mwasilu, F., & Jung, J. W. (2018). Effective protection for doubly fed induction generator-based wind turbines under three-phase fault conditions. *Electrical Engineering*, 100(2), 543-556. doi:10.1007/s00202-017-0528-0

MATLAB. (2021). Version 9.11 (R2021b). The MathWorks Inc.

Mohamed, S. A., & Abd El Sattar, M. (2019). A comparative study of P&O and INC maximum power point tracking techniques for grid-connected PV systems. *SN Applied Sciences*, *1*(2), 174. doi:10.1007/s42452-018-0134-4

Mwakijale, J. S., & Hilleringmann, U. (2024, October). Is AC or DC Distribution Line the Way Forward for Solar Swarm Grid Implementation? In *2024 IEEE PES/IAS PowerAfrica* (pp. 1-4). IEEE.

doi:10.1109/PowerAfrica61624.2024.10759435

Mwakijale, J. S., Safin, K. H., & Hilleringmann, U. (2024, October). Smart and Low-Cost Transceiver for Energy Sharing and Billing in the Implementation of Swarm Grids. In *2024 IEEE PES/IAS PowerAfrica* (pp. 1-4). IEEE. doi: 10.1109/PowerAfrica61624.2024.10759508

Mwakijale, J. S., Mwammenywa, I., & Hilleringmann, U. (2023, November). LoRa-based Swarm Grid Implementation for Rural Electrification in Africa. In *2023 IEEE PES/IAS PowerAfrica* (pp. 1-4). IEEE. doi:10.1109/PowerAfrica57932.2023.10363319

Mwammenywa, I., & Hilleringmann, U. (2023). Analysis of Electricity Power Generation and Load Profiles in Solar PV Microgrids in Rural Villages of East Africa: Case of Mpale Village in Tanzania. In *2023 IEEE AFRICON, Nairobi*. doi:10.1109/AFRICON55910.2023.10293635

Namujju, L. D., Mwammenywa, I., Kagarura, G. M., Hilleringmann, U., & Hehenkamp, B. (2024, March). Smart Metering and Choice Architecture in Demand-Side Management: A Power Resource-Constrained Perspective. In *2024 IEEE 8th Energy Conference (ENERGYCON)* (pp. 1-6). IEEE. doi:10.1109/ENERGYCON58629.2024.10488738

NASA - Langley Research Center. (n.d.). *Prediction of Worldwide Energy Resources (POWER)* (Hourly 2.x.x version). Retrieved August 27, 2024, from https://registry.opendata.aws/nasa-power

Peters, J., Sievert, M., & Toman, M. A. (2019). Rural electrification through mini-grids: Challenges ahead. *Energy Policy*, *132*. doi:10.1016/j.enpol.2019.05.016

Philipo, G. H., Jande, Y. A. C., & Kivevele, T. (2020). Demand-Side Management of Solar Microgrid Operation: Effect of Time-of-Use Pricing and Incentives. *Journal of Electrical and Computer Engineering*, *2020*, 6956214. doi:10.1155/2020/6956214

Sheridan, S., Sunderland, K., & Courtney, J. (2023). Swarm electrification: A comprehensive literature review. *Renewable and Sustainable Energy Reviews*, *175*, 113157. doi:10.1016/j.rser.2023.113157

Solcast. (2025). *Historical Time Series and Weather Data API*. Retrieved from Solcast website (historical time series documentation) on August 27, 2024.

Soltowski, B., Campos-Gaona, D., Strachan, S., & Anaya-Lara, O. (2019). Bottom-up electrification introducing new smart grids architecture-concept based on feasibility studies conducted in Rwanda. *Energies*, *12*(12). doi:10.3390/en12122439

SWARM-E Project. (n.d.). *Project Technology*. Retrieved August 27, 2025, from https://swarm-e.eu/technology/

Thompson Power Systems. (n.d.). Extending the life span of your diesel generator. Retrieved from https://thompsonpowersystems.com/resources/blog/extending-the-life-span-of-your-diesel-generator/

UNCTAD. (n.d.). *Commodities at a glance: Special issue - Access to energy in sub-Saharan Africa*. United Nations Conference on Trade and Development. Retrieved from https://unctad.org/publication/commodities-glance-special-issue-access-energy-sub-saharan-africa

United Nations. (2015). *Goal 7: Ensure access to affordable, reliable, sustainable and modern energy for all*. https://sdgs.un.org/goals/goal7

Varun. (2025). Renewable energy-based microgrid power management system. *International Journal of Electrical Power and Energy Systems (IJEPES)*, *2*(1), 1-23. doi:10.34218/IJEPES_02_01_001

Williams, N. J., Jaramillo, P., Campbell, K., Musanga, B., & Lyons-Galante, I. (2018, June). Electricity consumption and load profile segmentation analysis for rural micro grid customers in Tanzania. In *2018 IEEE PES/IAS PowerAfrica* (pp. 360-365). IEEE. doi:10.1109/PowerAfrica.2018.8521099